The On-Orbit Maneuvering of Large Space Flexible Structures by Free-Flying Robots

Yoshiyuki Ishijima[(1)], Dimitrios Tzeranis[(2)], Steven Dubowsky[(2)]

(1) Japan Aerospace Exploration Agency, 2-1-1, Sengen, Tsukuba, Ibaraki, 305-8505, Japan, ishijima.yoshiyuki@jaxa.jp
(2) MIT, 77 Massachusetts Avenue #3-469, Cambridge, MA 02139, USA, tzeranis@mit.edu,dubowsky@mit.edu

Keywords: Large space flexible structures, on-orbit maneuvering, space robotics

Abstract

This paper addresses the problems of planning and control of the on-orbit maneuvering of large and highly flexible structures by free-flying robots. An approach is proposed where the robots use their thrusters to control the "rigid body" motion of the robot-structure system being transported and their manipulators to control and damp out vibration in the structure induced by the thruster firings. A modal active damping control law is developed, which uses measurements of the structure state provided by free-flying sensing robots. Simulation results show that this approach is effective in transporting the structure into its desired position while using less fuel compared to suppressing vibration by the robot thrusters.

1. Introduction

The International Space Station (ISS) is an example of a large space structure (LSS) which has been constructed by assembling large modules in space by astronauts. Future space structures, such as proposed for space solar power plant systems, will be much larger and complex than ISS. The concept of space solar power system shown in Fig.1 is several kilometers across its largest dimension and is composed of extremely flexible structural modules. Such structures can only be assembled in-orbit. This construction would be too risky for astronauts. Teams of cooperative robots would be essential for on-orbit assembly.

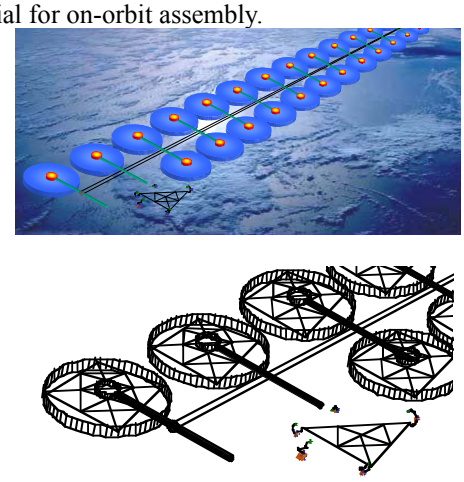

Fig.1 In-orbit construction of LSS by cooperative robots

It is assumed that the LSS construction is divided into three phases. The first phase is the assembly and/or deployment of substructure modules from some stowed configuration in the launch vehicle. The second phase is the maneuvering of the structural modules in the proximity of the main LSS (the structure under construction) by a team of free-flying robots, as illustrated in Fig.2. In the last phase, the module is assembled into the main LSS by a group of manipulators mounted on the main LSS. There are a number of challenges and technical problems of such robotic construction[1].

This paper focuses on control and planning of the maneuvering of large highly flexible structures by free-flying robots(Phase II). The large number of structure modules to be transported makes fuel consumption a critical issue. Since the robot thrusters are operated in a 'pulsed mode,' the optimum thrust force time profile for a minimum fuel maneuver is "bang-coast-bang." Such a force profile would cause large vibration displacements in the very flexible structure modules. Residual vibration should be minimized to make the module easier to be handled by the assembly manipulators after the maneuvering. Active modal damping by thrusters would result in additional fuel consumption. Furthermore, thrusters can not control a large number of vibration modes because of their limited bandwidth. This problem differs from the classic flexible structure slewing problem because robots use their manipulators to control the forces they apply to the structure[2],[3]. There have been studies on active damping by manipulators, but they do not discuss the active damping during thruster firings[4].

This paper describes a new approach using active modal damping by manipulators during on-orbit maneuvering. The approach which is called here a "decoupled controller" consists of a rigid motion controller using the robot's thrusters and a modal active damping controller using its manipulators. The two controllers act independently. The modal controller uses measurements of the structure state provided by free-flying sensing robots. Simulation results are presented that consider realistic constraints such as on/off thrusters, manipulator workspace and optimum thrust force input for fuel

consumption minimization. It is shown that cooperative robots can transport large flexible structures smoothly to a desired point in a specified time while using their manipulators to actively damp out vibration induced by the pulsed thrust forces.

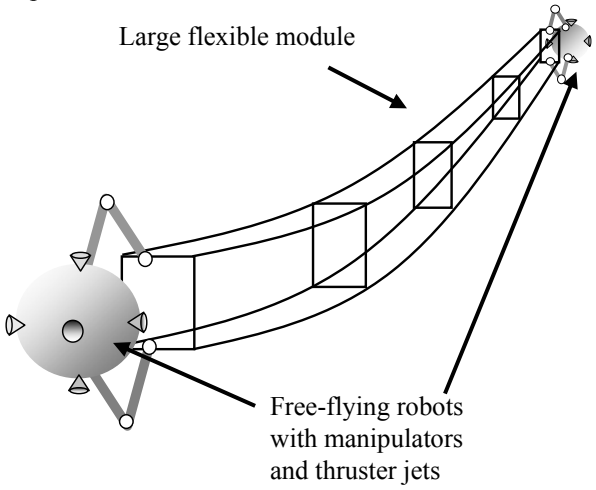

Fig.2 Maneuvering of a flexible structure by cooperative robots

2. System Models

The beam-like structure is transported by two robots equipped with thrusters and manipulators as illustrated in Fig.3. The two robots grasp the structure module at the ends. Observer robots provide modal estimation using cameras or laser range sensors. The robots are assumed to be equipped with thruster jets and manipulators.

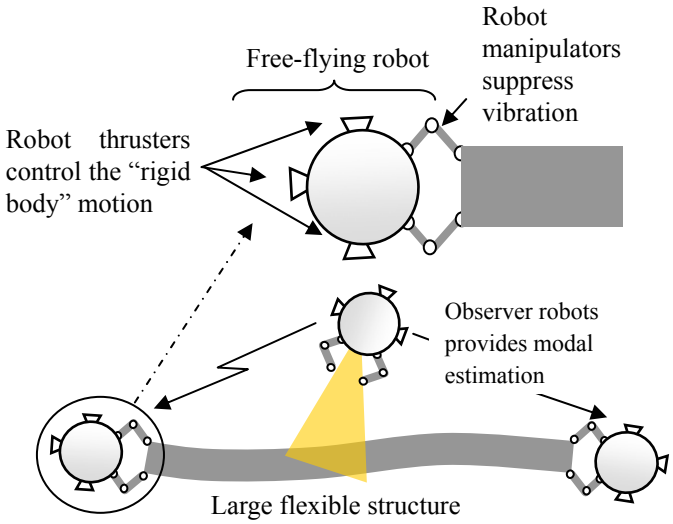

Fig.3 Maneuvering of a large flexible structure by two cooperative robots

A typical LSS structural module to be transported is a beam-like truss structure (Fig.4). The structure is modeled as a uniform Euler Bernoulli beam using Hamilton's principle.

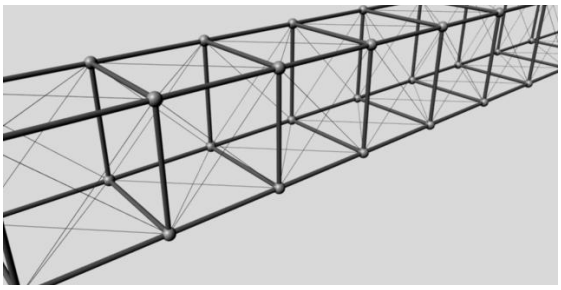

Fig.4 Beam-like truss structure module

The linearized equations of motion can be written as follows:

$$\underline{M}_m \cdot \ddot{\mathbf{x}}_b + \underline{C}_m(\mathbf{x}_b, \dot{\mathbf{x}}_b) \cdot \dot{\mathbf{x}}_b = \mathbf{W} \cdot \sum_i^n \mathbf{F}_{mp,i} \quad (1)$$

$$\ddot{\mathbf{q}} + 2 \cdot \underline{Z} \cdot \underline{\Omega} \cdot \dot{\mathbf{q}} + \underline{\Omega}^2 \cdot \mathbf{q} = \mathbf{B}_m \cdot \sum_i^n \mathbf{F}_{mp,i} \quad (2)$$

where $\mathbf{x}_b \equiv [\mathbf{r}_b, \theta_b]$ describes the rigid body motion of the structure (center of mass position and attitude) as illustrated in Fig.5. The vector $\mathbf{q}$ is composed of modal coordinates, $\mathbf{F}_{mp,i}$ contains the forces applied by the robots to the structure and n is the number of robots which perform maneuvering. Eq.(1) describes the module rigid body dynamics, and Eq.(2) describes its vibration dynamics.

Fig.5 shows the kinematic model of the system. The robot size is assumed to be small compared to the module. Therefore the robot bodies are modeled as point masses and the mass of manipulators is neglected. The centrifugal and coriolis forces are neglected due to the relatively slow angular rates of the system.

The robot equations of motion are:

$$m_{r,i}\ddot{\mathbf{r}}_{r,i} = \mathbf{F}_{th,i} - \mathbf{F}_{mp,i} - m_{r,i}\left(\ddot{\mathbf{r}}_b + \boldsymbol{\varphi}_i^T \ddot{\mathbf{q}} + 1/2\, L\ddot{\theta}_b\right) \quad (3)$$
$$\mathbf{F}_{th,i} = [F_{th,xi}, F_{th,yi},]^T, \mathbf{F}_{mp,i} = [F_{mp,xi}, F_{mp,yi},]^T$$

where $\mathbf{r}_{r,i} = [r_{r,x,i}, r_{r,y,i}]^T$ is the robot position, $m_{r,i}$ is the robot mass, $\mathbf{r}_b$ is the position of the beam center of mass, $\boldsymbol{\varphi}_i$ is the mode shape of the module at the grasping point, L is the length of the module, $\mathbf{F}_{th,i}$ is the thrust force applied by the robot jets and $\mathbf{F}_{mp,i}$ is the interaction force the robot and structure. The robot dynamics in Eq.(3) are expressed with respect to the non-inertial coordinate system which is fixed to the grasping point of the module, as shown in Fig.5.

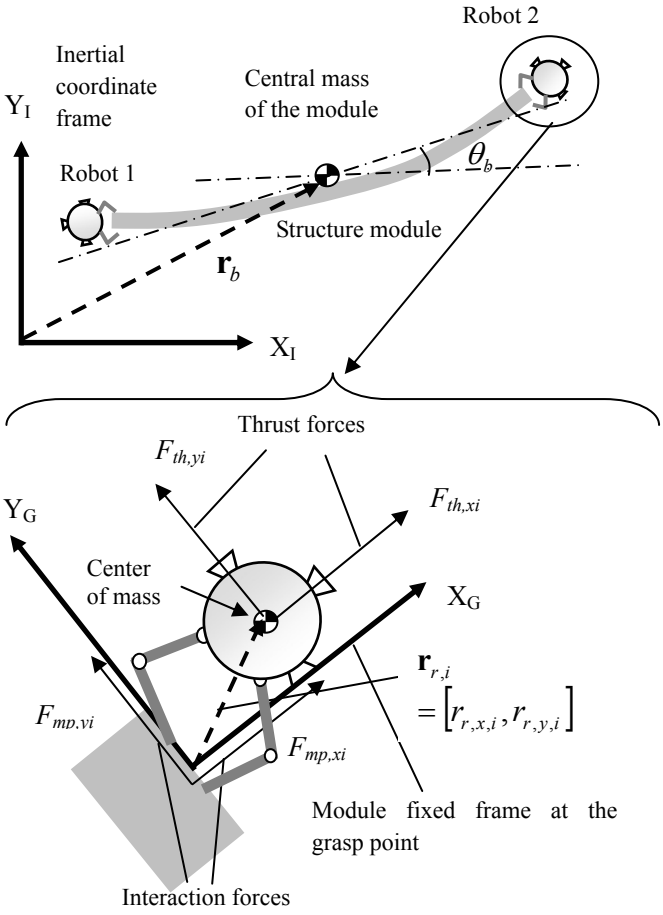

Fig.5 Kinematic model of the system

3. Controller Design

The proposed "decoupled controller" consists of two loops as shown Fig.6. The inner loop is an active modal damping controller for the interaction forces $\mathbf{F}_{mp,i}$ that damps out the structure vibration using the robots' manipulators. The outer loop is a 'rigid body motion' controller for the position and altitude of the robot-structure system that controls the robot thrusters.

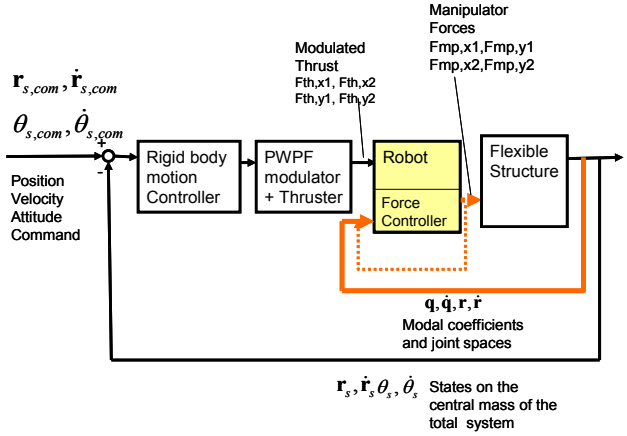

Fig.6 "Decoupled controller" block diagram

Active Modal Damping Using the Robot's Manipulators

The inner loop of the proposed algorithm controls the the y-component of the robot-structure interaction forces $\mathbf{F}_{mp,y}$ (direction of $\mathbf{Y}_G$ in Fig.5).

$$\mathbf{F}_{mp,y} = \mathbf{K}_\mathbf{r}\left(\mathbf{r}_{r,y} - \mathbf{r}_{ref,y}\right) + \mathbf{B}_\mathbf{r}\left(\dot{\mathbf{r}}_{r,y} - \dot{\mathbf{r}}_{ref,y}\right) + \mathbf{K}_\mathbf{q}\mathbf{q} + \mathbf{B}_\mathbf{q}\dot{\mathbf{q}} \quad (4)$$

where $\mathbf{r}_{r,y} = [r_{r,y,1}, \cdots, r_{r,n,y}]$ is the vector of the y-components of each robot position in Fig.4 and $\mathbf{q}$ is the modal coefficients of vibration. The gains $\mathbf{K_r}$ and $\mathbf{B_r}$ can be thought of as the stiffness and the damping factor of an imaginary spring and dashpot that connect the robot to the structure. $\mathbf{K_q}$ and $\mathbf{B_q}$ are the feedback gains of the active modal damping terms that control the module vibration. The feedback gains $\mathbf{K}_\mathbf{r}, \mathbf{B}_\mathbf{r}, \mathbf{K}_\mathbf{q}$ and $\mathbf{B}_\mathbf{q}$ are found by solving a Riccati equation so that the performance index J is minimized. The commands for the robot position and velocity $\mathbf{r}_{ref,y}, \dot{\mathbf{r}}_{ref,y}$ are zero.

$$\mathbf{K}_\mathbf{r}, \mathbf{B}_\mathbf{r}, \mathbf{K}_\mathbf{q}, \mathbf{B}_\mathbf{q} \rightarrow \min J, J = \int_0^\infty \left(\mathbf{x}^T\mathbf{Q}\mathbf{x} + \mathbf{u}^T\mathbf{R}\mathbf{u}\right)dt \quad (5)$$

where $\mathbf{Q}, \mathbf{R}$ are diagonal gain matrixes, $\mathbf{x} = \left[\mathbf{r}_{r,y}{}^T, \dot{\mathbf{r}}_{r,y}{}^T, \mathbf{q}^T\dot{\mathbf{q}}^T\right]^T$ is a state vector, and $\mathbf{u} = \mathbf{F}_{mp,y} = [F_{mp,y1}, \cdots, F_{mp\_yn}]$ are the y-directional forces applied by the manipulators to the structure. The controller uses the structure states $\mathbf{q}$ measured by free-flying observer robots[5]. The position of the robot $\mathbf{r}_{r,y}$ can be easily estimated from measurements of the manipulators joint angles. The x-components of the robot-structure interaction force $F_{mp,xi}$ are controlled using only $\mathbf{K_r}$ and $\mathbf{B_r}$ terms since it is assumed that they don't significantly influence the module vibration response.

Rigid Body Motion Controller Using the Robots' Thrusters

The robot-structure system can be described by the position of its center of mass and by the angle θ_s. The position and velocity of the robot-structure center of mass is:

$$\mathbf{r}_s = m_b\mathbf{r}_b + \sum_i^n m_{r,i}\mathbf{r}_{ri,i} \quad (6)$$

$$\mathbf{r}_{ri,i} = \mathbf{r}_{r,i} + \mathbf{r}_{g,i} + \mathbf{r}_b \quad (7)$$

$\mathbf{r}_{g,i}$ is the position vector from the structure center of mass to the grasping point and L is the length of the module. $\mathbf{r}_{g,i}$ can be written if the two robots grasp the module ends:

$$\mathbf{r}_{g,i} = 1/2L\left[(-1)^i \cos(\theta_b),(-1)^i \sin(\theta_b)\right]^T + \varphi_i{}^T \mathbf{q} \quad (8)$$
$$i = 1,2$$

The rate of change of θ_s is:

$$\dot{\theta}_s = \frac{I_{zz}\dot{\theta}_b + \sum_i^2 L/2 \cdot m_{r,i}\dot{\mathbf{r}}_{rI,i}}{I_{zz} + \sum_i^2 1/2\, m_{r,i}(L/2)^2} \quad (9)$$

where m_b is the mass of the flexible structure, $m_{r,i}$ is the mass of the each robot and I_{zz} is the moment of inertia of the structure. The command signals for the position and altitude of the robot-structure system $\mathbf{r}_{s,com}, \dot{\mathbf{r}}_{s,com}, \theta_{s,com}, \dot{\theta}_{s,com}$ are derived by solving an optimization problem to minimize the fuel consumption for the maneuver. The actual position and velocity rs, θ_s are controller by a "rigid body" closed-loop controller (outer loop of Fig.6), which consists of a position control loop and an attitude control loop. The design of this controller doesn't take into consideration the flexibility of the structure. The outer control loop output is converted into a thrust command by a pulse–width and pulse frequency modulation (PWPF)[6] which is commonly applied for satellites.

4. Simulation

Two robots, whose masses are 100kg, are assumed to grasp the mode at the ends. The module vibration is described by the first seven vibration modes. The thrusters are assumed to generate a pulsed 20 N force and are driven by the PWPF modulation. The feedback gains ***Q*** and ***R*** for the design of the active modal damping scheme are determined so that vibration is damped out and the robots remain within their joint space limits. ***R*** is the cost function for interaction forces.

Assuming that the motion of x-component (along the $\mathbf{X}_G$ direction of Fig.5) is small, the constraints on joint spaces can be written as a function of $\mathbf{r}_{r,y} = \left[r_{r,y,1}, r_{r,y,2}\right]$. The feedback gains of $\mathbf{K_r}$ and $\mathbf{B_r}$ are determined so that $r_{r,y,1}$ and $r_{r,2,y}$ avoid any singularities. The elements of ***Q*** are chosen considering the maximum values of $r_{r,y,1}$ and $r_{r,2,y}$, and vibration suppression performance. The parameters used in the simulations are shown in Table 1.

Using these parameters of **Q** and **R**, the feedback gain matrix of $\mathbf{K_r}, \mathbf{B_r}, \mathbf{K_q}$ and $\mathbf{B_q}$ are calculated as follows:

$$\mathbf{K_r}(N/m) = \begin{bmatrix} -89.4 & -0.042 \\ 0.042 & -89.4 \end{bmatrix} \quad (10)$$

$$\mathbf{B_r}(N/(m/s)) = \begin{bmatrix} -211.4 & -86.0 \\ -85.8 & -211.4 \end{bmatrix} \quad (11)$$

$$\mathbf{K_q}(N/m) = \begin{bmatrix} 21.9 & -4.13 & -2.30 & -8.60 & -4.88 & -9.40 & -5.21 \\ 21.9 & 4.15 & -2.32 & 8.68 & -5.29 & 9.96 & -6.88 \end{bmatrix} \quad (12)$$

$$\mathbf{B_q}(N/(m/s)) = \begin{bmatrix} -33.1 & -12.5 & -40.4 & -15.8 & -41.2 & -15.1 & -43.0 \\ -33.1 & 12.6 & -40.5 & 16.6 & -42.0 & 19.3 & -46.0 \end{bmatrix} \quad (13)$$

Table 1: Simulation parameters

Parameters	Values
Flexible Module	Mass m_b :600kg, Length L : 200m, Inertia I_{zz} : 2×10^6 kg m^2 Natural frequencies: 0.20, 0.55, 1.08, 1.78, 2.67, 3.75, 5.02Hz (Seven modes are considered)
Robot	Mass m_r :100kg
Thrusters	Thrust F_{max} : ±20N or 0 N (X_G, Y_G direction) Minimum ON/OFF time : 50msec Response delay : 50msec
Manipulators	Length : 1m + 1m (2-DOF)
Modal damping controller	Gain matrix for the states **Q** : $\mathbf{Q} = diag[Q_{1,1}, Q_{2,2} \cdots, Q_{18,18}]$ $Q_{1,1} = Q_{2,2} = 5.0\times10^7, Q_{3,3} = Q_{4,4} = 5.0\times10^5$ $Q_{5,5} = 10^7, Q_{6,6} = 10^6, Q_{7,7}, \cdots Q_{11,11} = 10^3$ $Q_{12,12} = 10^6, Q_{13,13} = 10^5, Q_{14,14}, \cdots Q_{18,18} = 10^3$ Gain matrix for the control variables **R** : $\mathbf{R} = diag[10^3, 10^3]$

4.1 A One Dimensional Maneuver Simulation Results

The performance of the controller is first evaluated through simulations of a simple one dimensional maneuver as shown in Fig.7. The corresponding optimum thrust force profile is a 'bang-coast-bang' profile shown in Fig.8. Fig.9 shows the vibration which is excited by a bang-coast-bang thrust force input. In this case, the robots are grasping the module firmly without providing active damping.

In this simulation, the proposed "decoupled controller" shown in Fig.6 is compared against a conventional "thrust only controller" in Fig.10, where vibration is damped out by only thruster jets. Fig 11 compares the fuel consumption for the one dimensional maneuver for the conventional controller and for the proposed controller. In case of the conventional controller, the thrust force profiles are different from the fuel-minimum solution (Fig. 12) because the robot uses its thrusters to damp out vibration. This affects the rigid body motion of the robot – structure system and causes increased fuel

consumption. In the proposed controller, robot manipulators do not attempt to control rigid body motion and contribute only to vibration suppression.

As long as robot manipulators move within their workspace shown in Fig.13, they can control vibration without any thruster actuation. When the acceleration maneuver starts, the robots move upward to reduce the displacement of the module. After finishing the maneuver, the robots move downward rapidly while pulling the end with a controlled interactive force, which also contributes to damping.

Thrusters have slow bandwidth due to minimum value of on/off switching time and time lags. Therefore, the thrust only control law can control only few low order modes. However, due to the higher bandwidth of manipulator actuators, the decoupled controller is able to damp out higher modes as shown in Fig.14. In this simulation, it is assumed that the modal coefficients are measured perfectly and can be obtained with a small delay (25msec). In a realistic situation, a sensing and estimation module of high bandwidth is necessary. This can be realized using accelerometers and vision sensors.

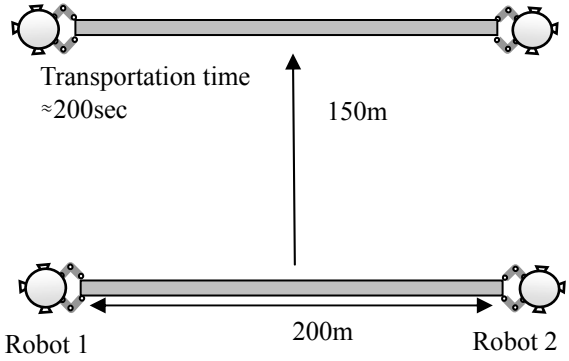

Fig.7 1-D structure transportation

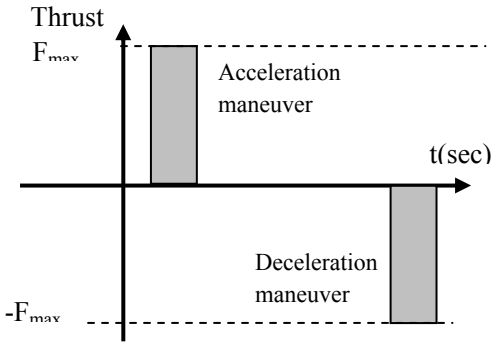

Fig.8 Bang-coast-bang force profile

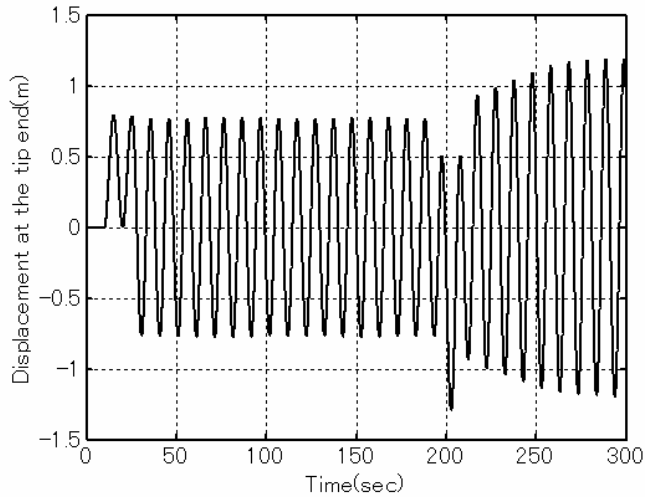

Fig.9 Exited vibration without active damping

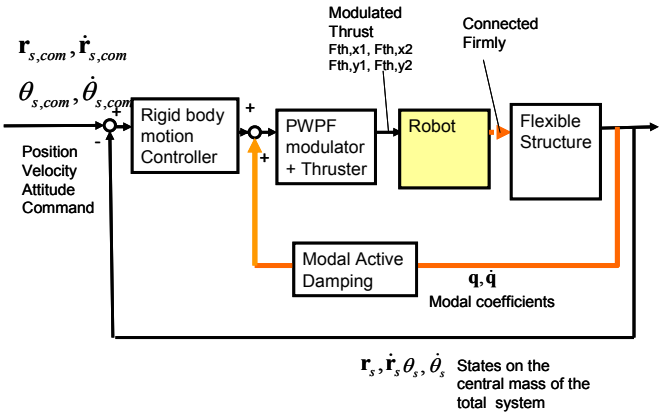

Fig.10 “Thrust only controller” block diagram

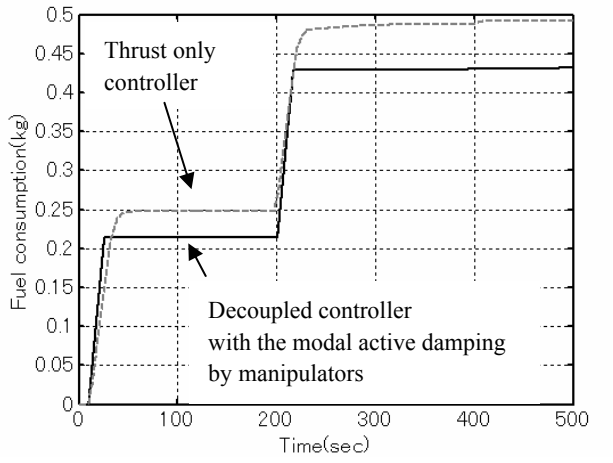

Fig.11 Fuel consumption of the two controllers

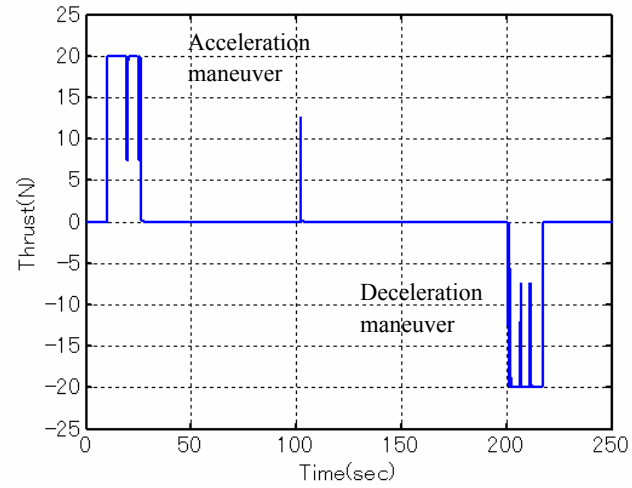

(a) Decoupled controller with active modal damping by manipulators

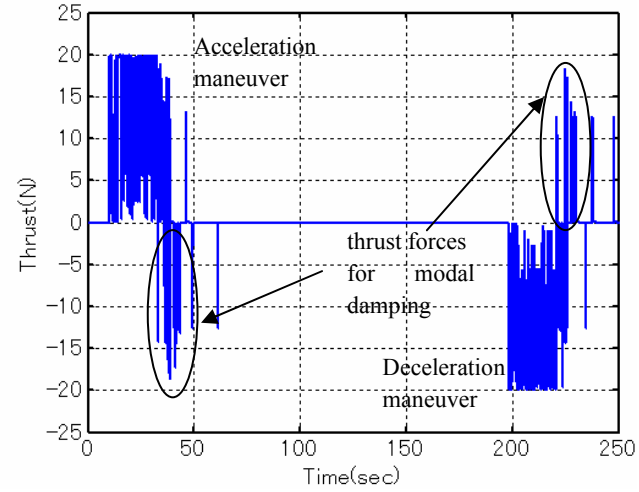

(b) Thrust only controller

Fig.12 Thrust force profile of the two controllers

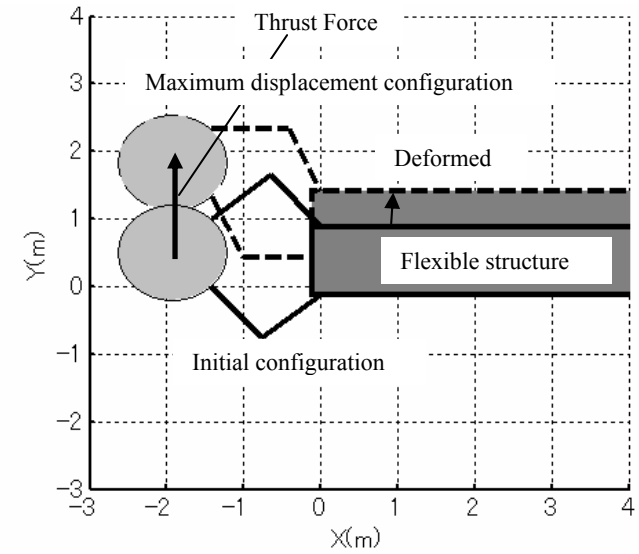

Fig.13 Motion of the robot 1 during acceleration

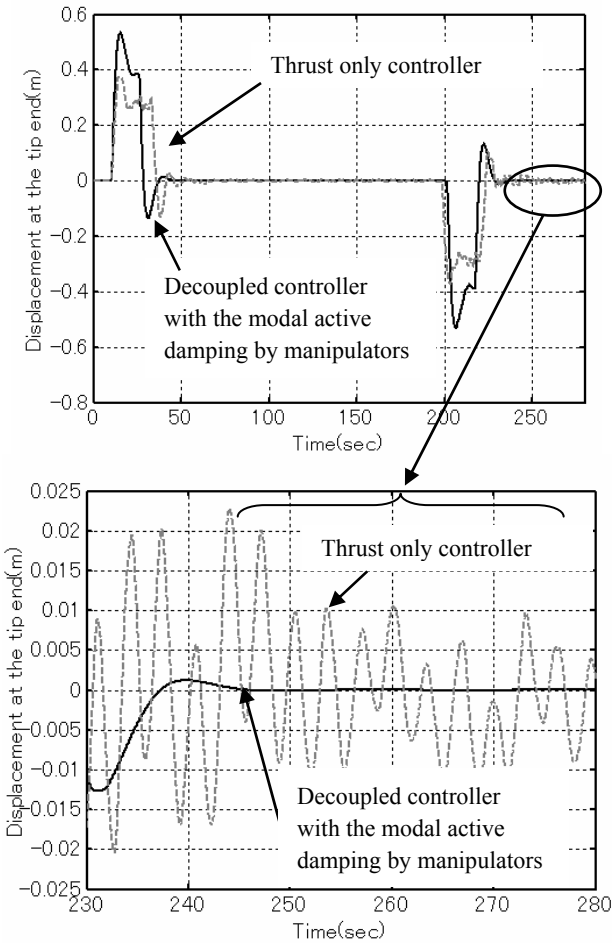

Fig.14 Residual vibration during transportation

4.2 Two Dimensional Transportation Maneuver Simulation Results

The performance of the decoupled controller for a two dimensional maneuver is evaluated. Fig.15 shows the case where the module is transported to the point of r_b=[150m, 150m] while it is rotated to an attitude of -90 degrees. The command for the rigid body motion of the robot-structure system is determined by solving an optimization problem to minimize fuel consumption. During the acceleration maneuver, the velocity is increased up to a desired value, and then the thrust is shut off. After the acceleration, it starts coasting. In the deceleration phase, the position and velocity are to be controlled to the specified final condition. A conventional dead-band controller is adopted to adjust them in the terminal phase. The attitude and attitude rate are controlled along the pre-determined commands by a PD controller all through the transportation.

This maneuver generates non-linear forces, such as centrifugal and Coriolis forces which would appear in Eq(3). Their magnitudes depend on the attitude rate $\dot{\theta}$. Assuming an average value of ω =0.5deg/s(=8.4 ×

10^{-3}rad/sec), the magnitudes of centrifugal and coriolis forces are estimated as $7.0\times10^{-1}N$ and $3.4\times10^{-1}N$ respectively. These forces are much smaller than the thruster forces(20N). Hence, they are modeled as disturbances.

Figure 16 shows the thrust forces and the interaction forces the robot's manipulators acting on the module. It can be seen that these forces are relatively small.

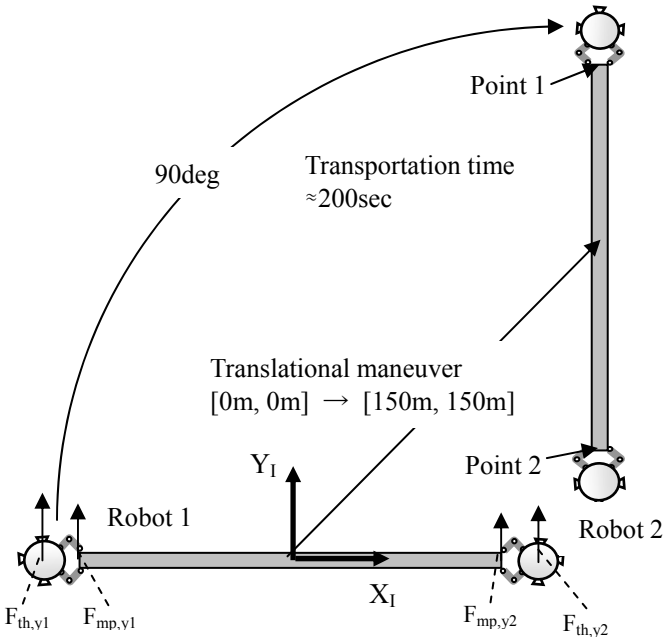

Fig.15 Schematic of a generic two dimensional transportation maneuver

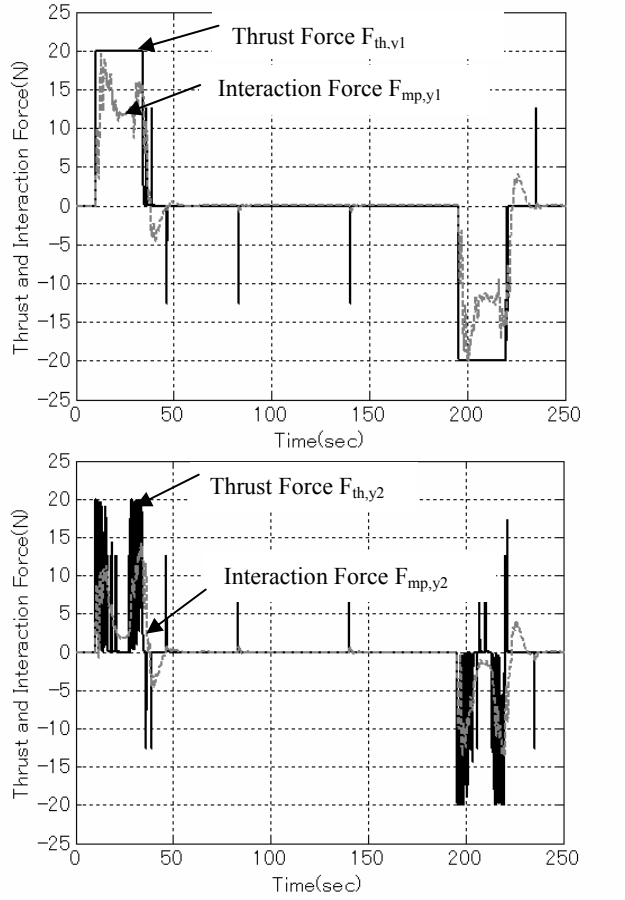

Fig.16 Thrust and interactive force profiles for the 2-D transportation maneuver

The displacement at the module end is shown in Fig.17. This figure shows that the decoupled controller performs well in damping out the vibration. The position error at this point is shown in Fig.18. The figures show the trajectories of the ends of the module in the terminal guidance. The terminal guidance by the conventional dead-band controller does not consider structural vibration. In the proposed approach, it works well because the manipulators can accommodate the flexibility. The module ends (Point 1 and Point 2) can be controlled to the desired points within the 2m radius circle with little vibration. The velocity error of the ends is approximately 2 cm/s. These position and velocity errors are small enough so that the manipulators on the main LSS can easily grasp the module to perform the final assembly.

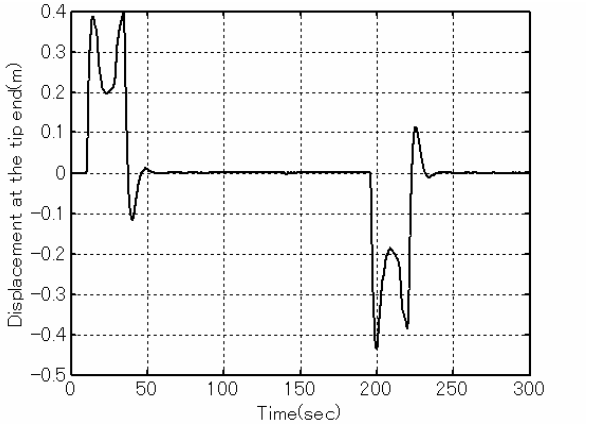

Fig.17 Displacement at the end of the module

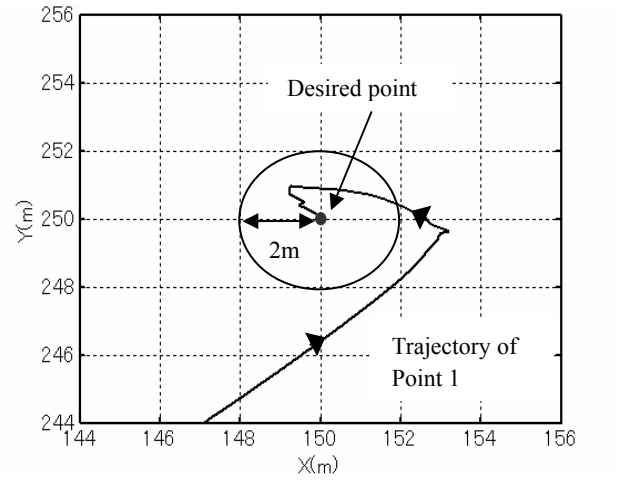

(a) Point 1

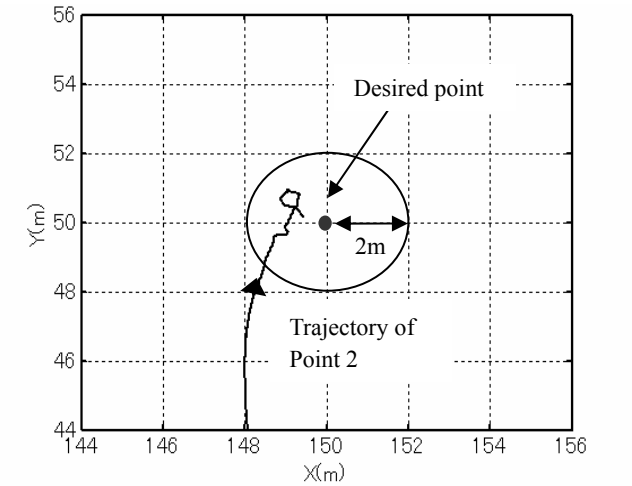

(b) Point 2

Fig.18 Trajectories of the ends of the module

5. Conclusions

This paper describes a large motion controller with active modal damping control law for the on-orbit maneuvering of flexible structures by robots with thrusters and manipulators. The controller performance is compared against a convectional controller that uses only thrusters. The results show that the controller with modal active damping using manipulators works well in damping out vibration without any additional fuel consumption during pulsed on-orbit maneuver. Furthermore, the robot based controller is able to control more effectively high vibration modes than using a simple transfer vehicle without manipulators. This suggests that robots may be more effective to transport large flexible structure on-orbit than simple transfer vehicles.

Acknowledgement

The authors would like to acknowledge JAXA for their support of this work, and Dr. Yoshiaki Ohkami, Dr. Mitsushige Oda and Mr. Hiroshi Ueno for helpful feedback during the development of this work.

References

1. Oda, M., and Mori, M., “Stepwise Development of SSPS; JAXA’s Current Study Status of the 1GW Class Operational SSPS and Its Precursor”, IAC-03-R.3.03, 54th International Astronautical Congress, Bremen, German, September-October, 2003

2. Singhose W. and Okada H., “Control of Flexible Satellites Using Analytic On-Off Thruster Commands”, Proceedings of the 2003 AIAA Guidance, Navigation and Control Conference.

3. Bennett, H.W., LaVigna, C., et al. “Nonlinear and Adaptive Control of Flexible Space Structures”, Transaction of the ASME, Vol.115, pp86-94, March, 1993.

4. Torres, A.M. and S. Dubowsky, “Vibration Control of Deployment Structures’ Long-Reach Manipulators: The P-PED Method” Proceedings of the 1996 IEEE International Conference on Robotic and Automation, Minneapolis, MI, April 1996.

5. Lichter, M.D. and S. Dubowsky, "State, Shape, and Parameter Estimation of Space Objects from Range Images." Proceedings of the 2004 IEEE International Conference on Robotics and Automation (ICRA 2004), New Orleans, LA, April 2004

6. Bitter, H., Fisher, H., and Surauer, M. “Design of Reaction Jet Attitude Control Systems for Flexible Spacecraft”, IFAC Automatic Control in Space, Noordwijk, Netherlands, IFAC, pp.373-98, 1982.